Superparamagnetism Found in Diluted Magnetic Semiconductor Nanowires: Mn-Doped CdSe

Chih-Chang Chen,[†] Yung-Jung Hsu,*[,‡] Yi-Feng Lin,[†] and Shih-Yuan Lu*[,†]

Department of Chemical Engineering, National Tsing Hua University, Hsinchu, Taiwan 30013, Republic of China, and Department of Materials Science and Engineering, National Chiao Tung University Hsinchu, Taiwan 30010, Republic of China

Received: August 6, 2008; Revised Manuscript Received: September 15, 2008

Diluted magnetic semiconductor (DMS) nanowires (NWs), Mn-doped CdSe, were successfully prepared in a gold-catalyzed vapor-transport deposition process. It was demonstrated for the first time that upon incorporation of Mn of very limited concentrations, the CdSe NWs exhibited enhanced ferromagnetism at $T < 40$ K and turned superparamagnetic at relatively high temperatures. This finding would extend the application range of DMS NWs into the biolabeling and bioimaging fields.

Introduction

One-dimensional (1D) semiconductor nanomaterials have drawn much research attention in the past decade because of their unique anisotropic characteristics in thermal, optical, and electrical properties, from which promising applications in fluorescence, optoelectronics, lasing, and sensing can be derived.[1] Recently, a tremendous amount of research effort has been undertaken to incorporate paramagnetic ions into 1D semiconductor nanostructures for possible applications in spintronics and quantum interference information processing.[2] These nanostructures belong to the family of diluted magnetic semiconductors (DMSs), in which the sp−d exchange interactions between the host semiconductor and the paramagnetic dopant result in unique magnetic and optomagnetic properties.[3] Presently, 1D nanostructures of Mn-doped II−VI and III−V semiconductors, such as ZnO,[4] ZnS,[5] ZnSe,[6] CdS,[7] GaN,[8] and GaP,[9] have been synthesized and investigated for their induced ferromagnetism at elevated temperatures, a property critical to applications in spintronics. In this article, we reported a successful synthesis of single-crystalline Mn-doped CdSe nanowires (NWs) in a gold-catalyzed vapor-transport deposition process. These NWs exhibited not only the induced ferromagnetism but also the induced superparamagnetism, reported for the first time for DMS NWs. The superparamagnetism was induced with incorporation of only a very limited amount of Mn (<2%) in the CdSe NWs and was characteristic of relatively high transition temperatures. Superparamagnetic nanocrystals have been proven to be a very promising candidate for specific contrast agents in magnetic resonance and optical imaging, as they are not subject to strong magnetic interactions in dispersions.[10] The present finding extends the application range of DMS NWs into the biolabeling and bioimaging areas.

Experimental Methods

Chemicals. All chemicals used were analytic grade reagents and used without further purification. Special attention should be paid when dealing with the hazardous CdSe source.

Vapor-Transport Deposition for Preparation of Mn-Doped CdSe NWs. Mn-doped CdSe NWs were grown in a three-zone hot-wall reactor under a reduced pressure. Amorphous fused silica sputtered with a thin layer of gold was used as the substrate. The source material, CdSe and $MnCl_2$ powders, of appropriate amounts was contained in the quartz boats, which were separately placed at locations of temperatures 725 and 300 °C, respectively, to generate necessary vapors within the reactor. The vapors of CdSe and Mn condensed to crystallize on the fused silica substrate to form NWs at the deposition temperature of 350 °C. All depositions were run for 6 h with a carrier nitrogen gas flow rate of 100 sccm and a system pressure of 400 Torr. A postannealing treatment at 500 °C for 12 h in nitrogen atmosphere was then carried out for the as-deposited samples. The Mn incorporation level was controlled by the amount of $MnCl_2$ used in the deposition. The Mn concentrations of 0.4, 0.9, and 1.3 atom % were achieved with an amount of starting $MnCl_2$ of 0.1, 0.15, and 0.3 g, respectively.

Characterizations. The morphology and dimensions of the products were examined with a field-emission scanning electron microscope (FESEM, Hitachi S-4700). The crystallographic structure of the samples was investigated with X-ray diffraction (XRD, MAC Science MXP18), and a high-resolution TEM (HRTEM, JEOL JEM-3000) operated at 300 kV. The compositional information was obtained with an energy dispersive spectrometer (EDS), an accessory of the HRTEM (JEM-3000), and X-ray photoelectron spectroscope (XPS, VG Scientific, Microlab 350). Magnetization measurements of the samples were carried out at low temperatures by using a superconducting quantum interference device magnetometer (SQUID, Quantum Design, MPMS5). The externally applied magnetic field was perpendicular to the substrate plane. The magnetic signals arising from the substrate that supported the sample were deducted from the magnetization data reported. Magnetizations instead of specific magnetizations (magnetizations normalized with the sample mass) were reported since the amounts of NWs were too small to be accurately determined. This situation, however, did not affect the magnetic parameters that we collected and discussed in this work.

* Corresponding author. E-mail: yhsu@cc.nctu.edu.tw and sylu@mx.nthu.edu.tw.
[†] Department of Chemical Engineering, National Tsing Hua University.
[‡] Department of Materials Science and Engineering, National Chiao Tung University Hsinchu.

10.1021/jp807032q CCC: $40.75
Published on Web 10/24/2008

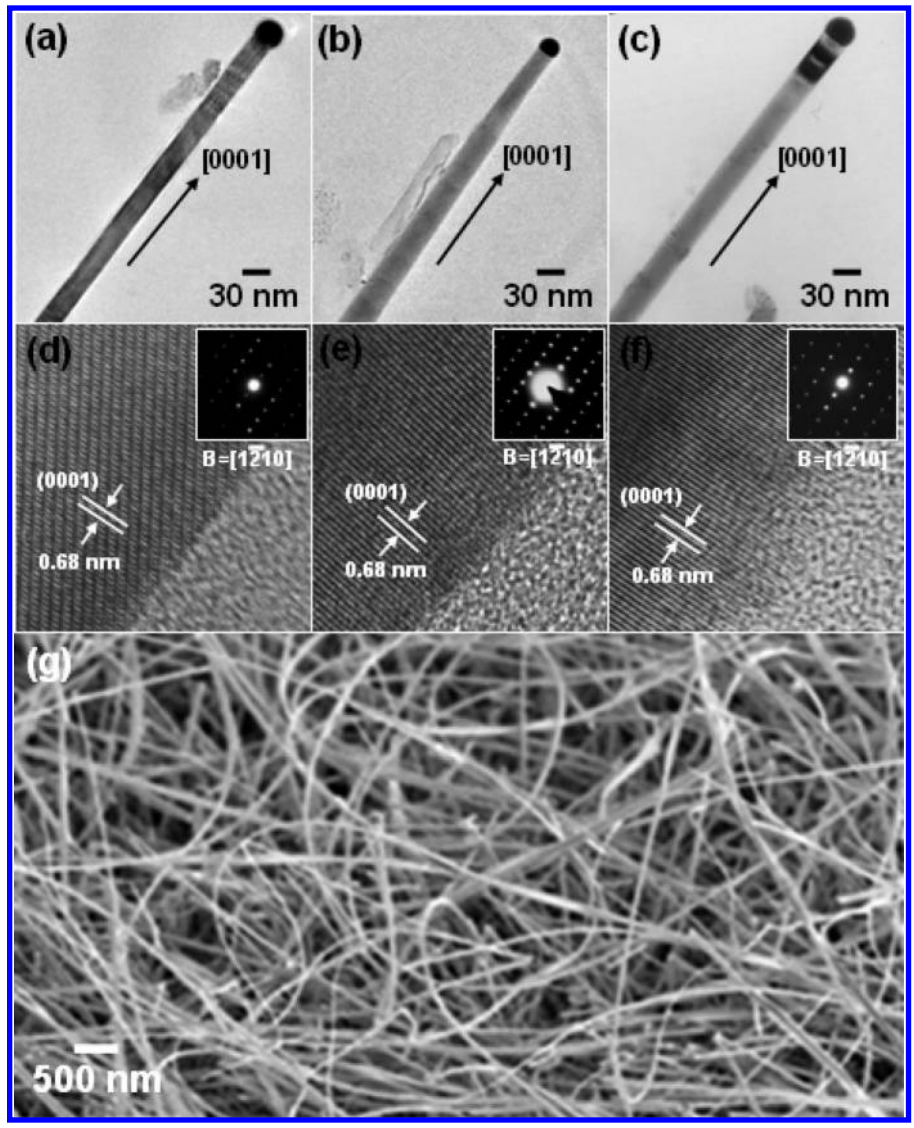

Figure 1. TEM images of CdSe NWs doped with Mn of (a) 0.4, (b) 0.9, and (c) 1.3 atom %. Their corresponding HRTEM and ED images were shown in panels d, e, and f, respectively. (g) SEM image of CdSe NWs doped with 1.3 atom % Mn.

Results and Discussion

Figure 1 shows the transmission electron microscope (TEM) images of the CdSe NWs, around 40 nm in diameter, doped with different amounts of Mn. The atomic concentrations of Mn in these NWs, as determined from the corresponding TEM-energy dispersive spectrometry (TEM-EDS), were 0.4, 0.9, and 1.3 atom % for samples a, b, and c, respectively. Figure 1g, a representative scanning electron microscope (SEM) image of the sample, shows the abundance and up to several micrometer lengths of the NWs. The clear lattice fringes present in panels d, e, and f of Figure 1 show the single-crystalline nature of the as-prepared NWs, which were further verified with the dot patterns of the corresponding electron diffraction (ED) images shown in the insets of Figure 1. The interlayer spacing of around 0.68 nm indicates a reasonable shrinkage in the *d* spacing of the (0001) lattice planes of the hexagonal CdSe crystal when Cd was partially replaced with Mn, which is of a smaller atomic size. The resolution of the HRTEM images, Figure 1d−f, however, was not enough to quantitatively differentiate the spacing difference resulting from the corresponding doping levels, while a qualitative trend can be concluded. Furthermore, the Mn-doped CdSe NWs grew along the *c*-axis, [0001], of the hexagonal crystalloid. The relatively large theoretical binding energy of Mn with the (0001) facet, as compared to those with other facets, of the hexagonal CdSe crystals[11] may favor the incorporation of Mn through the growth of the *c*-plane.

The XRD patterns of the as-synthesized undoped CdSe and Mn-doped CdSe NWs confirmed the hexagonal wurtzite phase of the products without formation of other impurity phases such as Cd or Mn oxides (Figure 2). The inset of Figure 2 displays the magnified (100), (002), and (101) diffraction peaks, showing the peak-shifting to higher 2θ regions with increasing Mn incorporation. The substitution of Cd atoms with smaller Mn atoms resulted in a reduction in the lattice constants and thus a peak shift to the higher 2θ region, consistent with the *d* spacing shrinkage observed in the HRTEM images. The amounts of peak shift can be further used to estimate the concentration of Mn through a linear relationship established based on previous data collected by Karande et al. from Mn-doped CdSe thin films.[12] The concentrations of Mn thus found for samples a, b, and c were 0.4, 0.8, and 1.4 atom %, respectively, in reasonably good agreement with those from the TEM-EDS measurements, implying a homogeneous distribution of Mn within the CdSe NWs. It may be argued that the XRD peak shifts may also result from core−shell nanostructures or even segregated MnSe phases for the present case, instead of the homogeneous distribution

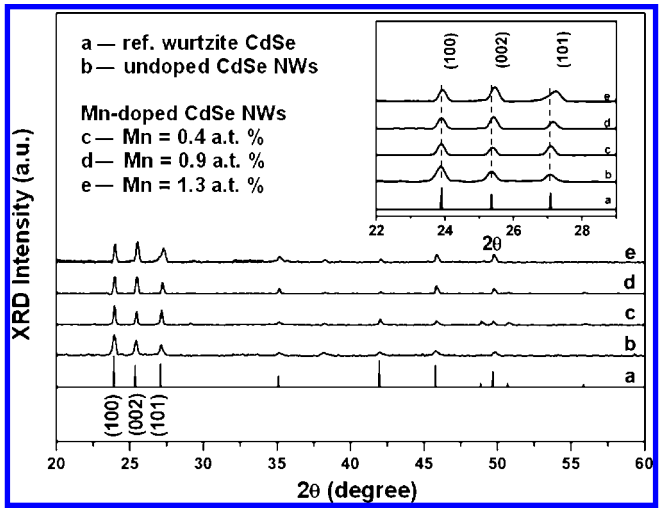

Figure 2. XRD pattern of undoped and Mn-doped CdSe NWs, compared with that of a reference wurtzite CdSe (JCPDS no. 08-0459).

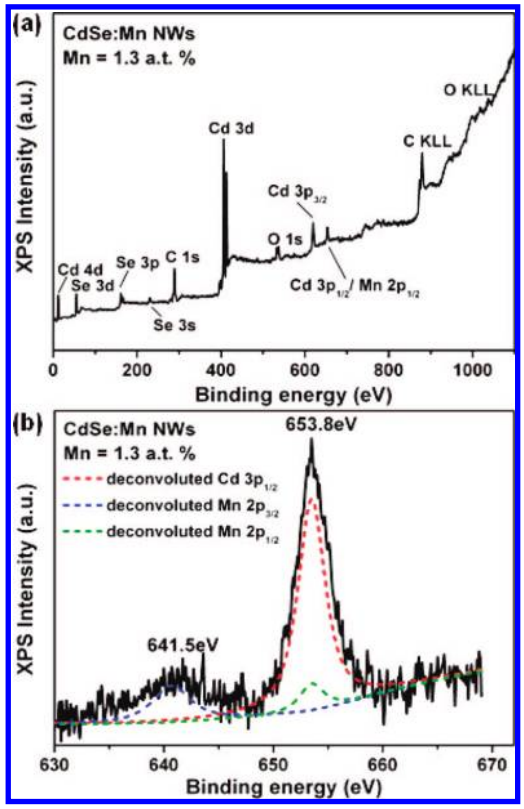

Figure 3. XPS spectra of CdSe NWs doped with 1.3 atom % Mn: (a) survey scan and (b) fine scan at the vicinity of 653 eV. Peak deconvolution in panel b revealed the presence of Cd $3p_{1/2}$, Mn $2p_{1/2}$, and Mn $2p_{3/2}$ peaks.

of Mn. From the HRTEM images, there were observed no core−shell structures and segregated phases, and thus these two possibilities can be ruled out. As a result, the concentration of the incorporated Mn and the resulting changes in lattice constants of the NWs obeyed the Vegard law.[13]

The chemical states of the as-synthesized products were analyzed with the X-ray photoelectron spectroscope (XPS) to investigate the binding state of the incorporated Mn. A survey scan taken on one of the doped samples (1.3 atom %) was shown in Figure 3a. As expected, there were present the Cd, Se, and Mn signals of correct binding energies. The peak of Cd $3p_{1/2}$ was found to overlap with that of Mn $2p_{1/2}$ since both of them

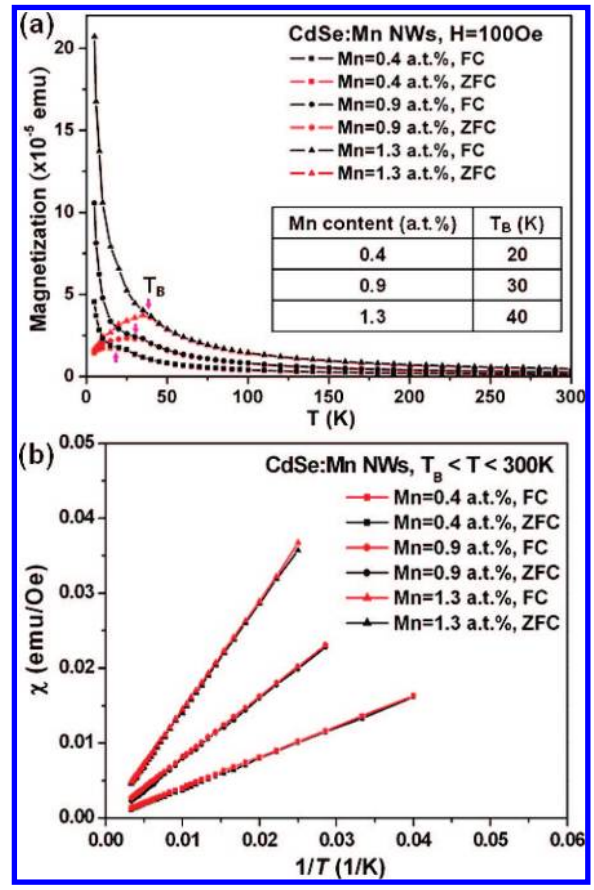

Figure 4. (a) Magnetization versus temperature curves conducted at a magnetic field of 100 Oe for Mn-doped CdSe NWs. The inset shows the blocking temperatures (T_B) of the samples of three different Mn doping levels. (b) Susceptibility (χ) versus $1/T$ plot for Mn-doped CdSe NWs conducted at a magnetic field of 100 Oe with the temperature ranging from the corresponding block temperatures to 300 K.

possessed binding energies of around 653 eV.[14,15] A finely scanned spectrum taken at the vicinity of 653 eV was shown in Figure 3b to further investigate the binding states of Mn. In Figure 3b, the peak deconvolution confirmed the merging of Cd $3p_{1/2}$ and Mn $2p_{1/2}$ peaks at the binding energy of 653.8 eV. Note that the Cd $3p_{1/2}$ peak predominated over the Mn $2p_{1/2}$ one due to the limited amount of Mn incorporation. Furthermore, the Mn $2p_{3/2}$ and Mn $2p_{1/2}$ peaks observed at the binding energies of 641.5 and 653.8 eV, respectively, revealed the presence of Mn−Se bonds in the doped NWs.[15] This result, together with those of HRTEM, TEM-EDS, and XRD analyses, confirmed the successful doping of Mn in the CdSe NWs forming the Mn−Se bridging domain instead of Mn−Mn clusters.

The magnetic property of the products was analyzed with a superconducting quantum interference device (SQUID) magnetometer. Figure 4a depicts the temperature-dependent magnetization data for the Mn-doped CdSe NWs measured with an applied field of 100 Oe. The data collected at the zero-field-cooled (ZFC) and field-cooled (FC) conditions exhibited a basic feature of superparamagnetism: a broad ZFC peak and its divergence from the FC curve below a critical temperature. The temperature at which the ZFC curve reaches its maximum is termed the blocking temperature, T_B.[16] At $T < T_B$, the divergence in the ZFC and FC curves is characteristic of the ferromagnetism, while at $T > T_B$, the complete overlap of the two curves implies a paramagnetic-like behavior. In addition, a linear relationship between the susceptibility and the reciprocal

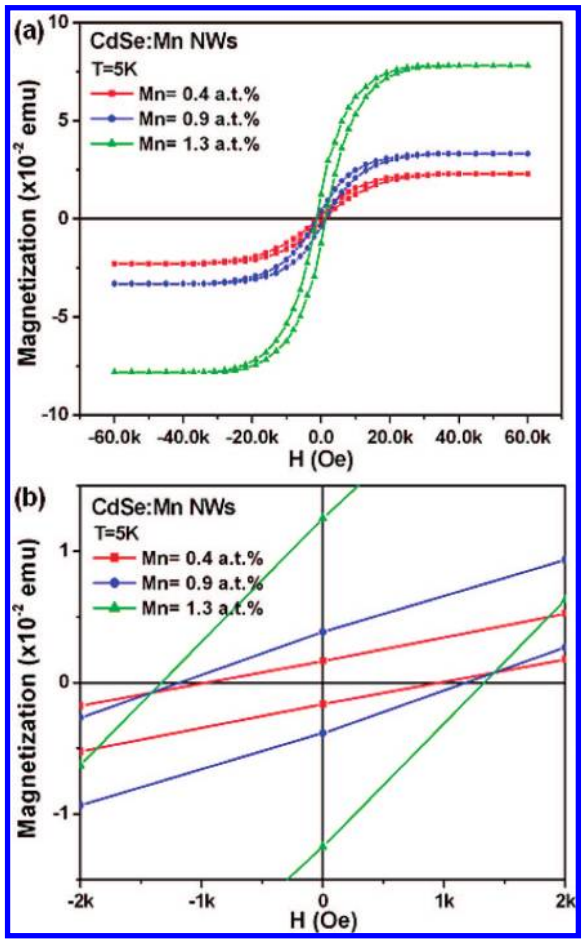

Figure 5. (a) Magnetization curves of Mn-doped CdSe NWs measured at 5 K. (b) The corresponding magnified curves in the vicinity of the origin.

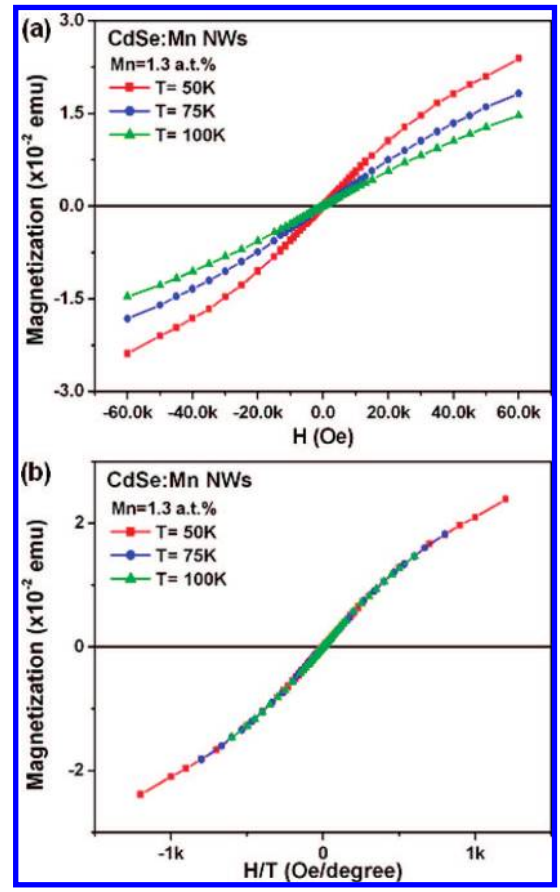

Figure 6. (a) Magnetization curves of Mn-doped CdSe NWs measured at 50, 75, and 100K. (b) The corresponding magnetization versus magnetic field/temperature plots.

of temperature was observed (Figure 4b), in agreement with the Curie law. This paramagnetic-like phenomenon was shown to be superparamagetism as discussed later. It should be noted that the T_B found here increased with increasing Mn concentration and were larger than that of the Mn-doped CdSe quantum dots.[17] As compared with quantum dot or thin film samples, the larger T_B observed in the present NW architecture implies larger magnetic anisotropy, and enhanced magnetic anisotropy has been commonly observed in 1D nanostructures because of the shape anisotropy.[18] Note that the ferromagnetism of doped NWs came from the Mn atoms possessing magnetic dipoles that are aligned in the same direction within the magnetic domains. The increase of Mn concentration led to the increasing coupling extent of the aligned dipoles within the magnetic domains. An enhanced resistance to thermal agitations was then achieved, leading to an increase of T_B with increasing Mn concentrations.

To further elucidate the nature of the magnetism observed in our samples, we performed SQUID measurements at different temperature regimes. Figure 5a shows the magnetization (M) versus magnetic field (H) plot recorded at 5 K, a temperature lower than the T_B of the three doped samples. All of the $M-H$ curves exhibited hysteresis, which is characteristic of ferromagnetism. Figure 5b displays the magnified $M-H$ curve in the vicinity of the origin, revealing the coercive fields of the samples. The coercivities of the samples increased with increasing Mn concentration (H_C = 960, 1179, 1331 Oe, for Mn = 0.4, 0.9, 1.3 atom %, respectively). As compared to the Mn-doped CdSe quantum dots,[17] enhanced coercive fields were obtained for our NW samples, consistent with the relevant comparison of T_B and demonstrating again the enhanced magnetic anisotropy commonly found in 1D nanostructures.[18]

The $M-H$ curves of these doped NW samples recorded at T = 50, 75, and 100 K, temperatures above their T_B, were shown in Figure 6a. Expectedly, the hysteresis phenomenon disappeared, suggesting superparamagnetism at temperatures higher than T_B. In fact, if one plots M versus H/T for the three samples, an excellent curve superimposition results as shown in Figure 6b, again indicating superparamagnetism.[16] It may be argued that the superparamagnetism found in the current work may arise from the possible formation of segregated MnSe phases or Mn/Au alloy at the tips of the CdSe NWs, instead of the incorporated Mn atoms. Note that MnSe exhibits antiferromagnetism at low temperatures,[19] and there has been observed no segregated MnSe phases in the NWs. As a result, the possibility that segregated MnSe phases contributed to the superparamagnetism can be ruled out. In addition, no detectable Mn was found at the Au tips of the CdSe NWs, and thus excluded the existence of the Mn/Au alloy. As a final note, no significant magnetization was found for the undoped CdSe NWs. As shown in Figure 7, the magnetization intensity was three orders of magnitude smaller than that of the doped CdSe NWs, confirming that the magnetism of the doped NWs came from the incorporated Mn.

Conclusions

In summary, DMS NWs of Mn-doped CdSe were successfully prepared in a gold-catalyzed vapor-transport deposition process. It was demonstrated for the first time that upon incorporation of Mn of a very limited amount, CdSe NWs exhibited enhanced

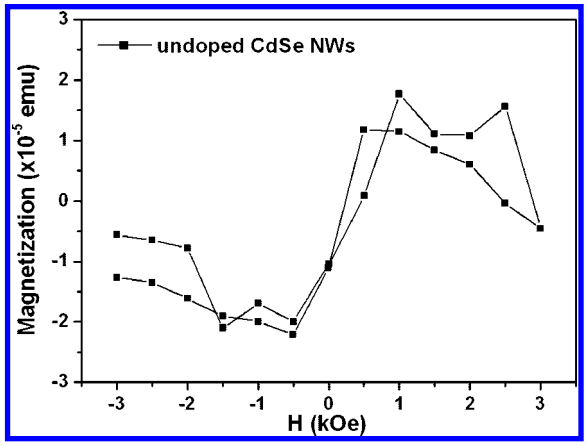

Figure 7. Magnetization curve of undoped CdSe NWs.

ferromagnetism at $T < 40$ K and turned superparamagnetic at relatively high temperatures. This finding would extend the application range of DMS NWs into the biolabeling and bioimaging fields.

Acknowledgment. This work was financially supported by the National Science Council of the Republic of China (Taiwan) under grants NSC-96-2218-E-009-007 (Y.-J.H.) and NSC-95-2221-E-007-194 (S.-Y.L.).

References and Notes

(1) (a) Murphy, C. J.; Sau, T. K.; Gole, A. M.; Orendorff, C. J.; Gao, J.; Gou, L.; Hunyadi, S. E.; Li, T. *J. Phys. Chem. B* **2005**, *109*, 13857. (b) Sirbuly, D. J.; Law, M.; Pauzauskie, P.; Yan, H.; Maslov, A. V.; Knudsen, K.; Saykally, R. J.; Yang, P. *Proc. Nat. Acad. Sci.* **2005**, *102*, 7800. (c) Pauzauskie, P.; Yang, P. *Mater. Today* **2006**, *9*, 36.

(2) (a) Pearton, S. J.; Norton, D. P.; Heo, Y. W.; Tien, L. C.; Ivill, M. P.; Li, Y.; Kang, B. S.; Ren, F.; Kelly, J.; Hebard, A. F. *J. Electron. Mater.* **2006**, *35*, 862. (b) Chikoidze, E.; Dumont, Y.; Von Bardeleben, H. J.; Gleize, J.; Jomard, F.; Rzepka, E.; Berrerar, G.; Ferrand, D.; Gorochov, O. *Appl. Phys. A: Mater. Sci. Process.* **2007**, *88*, 167.

(3) (a) Furdyna, J. K. *J. Appl. Phys.* **1988**, *64*, R29. (b) Ohno, H. *Science* **1998**, *281*, 951. (c) Ohno, Y.; Young, D. K.; Beschoten, B.; Matsukura, F.; Ohno, H.; Awschalom, D. D. *Nature* **1999**, *402*, 790. (d) Ohno, H.; Chiba, D.; Matsukura, F.; Omiya, T.; Abe, E.; Dietl, T.; Ohno, Y.; Ohtani, K. *Nature* **2000**, *408*, 944. (e) Dietl, T.; Ohno, H.; Matsukura, F.; Cibert, J.; Ferrand, D. *Science* **2000**, *287*, 1019.

(4) (a) Baik, J. M.; Lee, J.-L. *Adv. Mater.* **2005**, *17*, 2745. (b) Liu, L. Q.; Xiang, B.; Zhang, X. Z.; Zhang, Y.; Yu, D. P. *Appl. Phys. Lett.* **2006**, *88*, 063104. (c) Yuhas, B. D.; Zitoun, D. O.; Pauzauskie, P. J.; He, R.; Yang, P. *Angew. Chem., Int. Ed.* **2006**, *45*, 420.

(5) (a) Brieler, F. J.; Grundmann, P.; Froba, M.; Chen, L.; Klar, P. J.; Heimbrodt, W.; von Nidda, H.-A. K.; Kurz, T.; Liodl, A. *J. Am. Chem. Soc.* **2004**, *126*, 797. (b) Biswas, S.; Kar, S.; Chaudhuri, S. *J. Phys. Chem. B* **2005**, *109*, 17526.

(6) Lee, J. Y.; Kim, D. S.; Kang, J. S.; Yoon, S. W.; Lee, H.; Park, J. *J. Phys. Chem. B* **2006**, *110*, 25869.

(7) (a) Radovanovic, P. V.; Barrelet, C. J.; Gradecak, S.; Qian, F.; Lieber, C. M. *Nano Lett.* **2005**, *5*, 1407. (b) Na, C. W.; Han, D. S.; Kim, D. S.; Kang, Y. J.; Lee, J. Y.; Park, J.; Oh, D. K.; Kim, K. S.; Kim, D. *J. Phys. Chem. B* **2006**, *110*, 6699.

(8) (a) Choi, H.-J.; Seong, H.-K.; Chang, J.; Lee, K.-I.; Park, Y.-J.; Kim, J.-J.; Lee, S.-K.; He, R.; Kaykendall, T.; Yang, P. *Adv. Mater.* **2005**, *17*, 1351. (b) Han, S.-E.; Oh, H.; Kim, J.-J.; Seong, H.-K.; Choi, H.-J. *Appl. Phys. Lett.* **2005**, *87*, 062102.

(9) Han, D. S.; Bae, S. Y.; Seo, H. W.; Kang, Y. J.; Park, J.; Lee, G.; Ahn, J.-P.; Kim, S.; Chang, J. *J. Phys. Chem. B* **2005**, *109*, 9311.

(10) (a) Gu, H.; Xu, K.; Xu, C.; Xu, B. *Chem. Commun.* **2006**, 941. (b) Jun, Y. W.; Huh, Y. M.; Choi, J. S.; Lee, J. H.; Song, H. T.; Kim, S. J.; Yoon, S.; Kim, K. S.; Shin, J. S.; Suh, J. S.; Cheon, J. *J. Am. Chem. Soc.* **2005**, *127*, 5732. (c) Ge, J.; Hu, Y.; Biasini, M.; Beyermann, W. P.; Yin, Y. *Angew. Chem., Int. Ed.* **2007**, *46*, 4342.

(11) Erwin, S. C.; Zu, L.; Haftel, M. I.; Efros, A. L.; Kennedy, T. A.; Norris, D. J. *Nature* **2005**, *436*, 91.

(12) Karande, V. S.; Mane, S. H.; Pujari, V. B.; Deshmukh, L. P. *Mater. Lett.* **2005**, *59*, 148.

(13) Zhou, D.; Usher, B. F. *J. Phys. D: Appl. Phys.* **2001**, *34*, 1461.

(14) Qin, T.; Lu, J.; Wei, S.; Qi, P.; Peng, Y.; Yang, Z.; Qian, Y. *Inorg. Chem. Commun.* **2002**, *5*, 369.

(15) Bowen Katari, J. E.; Colvin, V. L.; Alivisatos, A. P. *J. Phys. Chem.* **1994**, *98*, 4109.

(16) Fonseca, F. C.; Goya, G. F.; Jardim, R. F.; Muccillo, R.; Carreño, N. L. V.; Longo, E.; Leite, E. R. *Phys. Rev. B* **2002**, *66*, 104406.

(17) Magana, D.; Perera, S. C.; Harter, A. G.; Dalal, N. S.; Strouse, G. F. *J. Am. Chem. Soc.* **2006**, *128*, 2931.

(18) (a) Deepak, F. L.; Vanitha, P. V.; Govindaraj, A.; Rao, C. N. R. *Chem. Phys. Lett.* **2003**, *374*, 314. (b) Roy, V. A. L.; Djuristic, A. B.; Liu, H.; Zhang, X.-X.; Leung, Y.-H.; Xie, M.-H.; Gao, J.; Lui, H.-F.; Surya, C. *Appl. Phys. Lett.* **2004**, *84*, 756.

(19) Squire, C. F. *Phys. Rev.* **1939**, *56*, 922.

JP807032Q